3-27-2018

Modeling of NiTiHf Using Finite Difference Method

Nazanin Farjam
The University of Toledo

Reza Mehrabi
The University of Toledo

Haluk E. Karaca
University of Kentucky, karacahaluk@uky.edu

Reza Mirzaeifar
Virginia Tech

Mohammad Elahinia
The University of Toledo

PROCEEDINGS OF SPIE

SPIEDigitalLibrary.org/conference-proceedings-of-spie

Modeling of NiTiHf using finite difference method

Nazanin Farjam, Reza Mehrabi, Haluk Karaca, Reza Mirzaeifar, Mohammad Elahinia

Nazanin Farjam, Reza Mehrabi, Haluk Karaca, Reza Mirzaeifar, Mohammad Elahinia, "Modeling of NiTiHf using finite difference method," Proc. SPIE 10596, Behavior and Mechanics of Multifunctional Materials and Composites XII, 1059613 (27 March 2018); doi: 10.1117/12.2300857

Event: SPIE Smart Structures and Materials + Nondestructive Evaluation and Health Monitoring, 2018, Denver, Colorado, United States

Modeling of NiTiHf using Finite Difference Method

Nazanin Farjam[a], Reza Mehrabi[a], Haluk Karaca[b], Reza Mirzaeifar[c], Mohammad Elahinia*[a]
[a]Mechanical, Industrial and Manufacturing Engineering (MIME) Department, University of Toledo, Toledo, OH USA 43606; [b]Dept. of Mechanical Engineering, University of Kentucky, Lexington, KY USA 40506; [c]Dept. of Mechanical Engineering, Virginia Tech, Blacksburg, VA USA 24061.

ABSTRACT

NiTiHf is a high temperature and high strength shape memory alloy with transformation temperatures above 100^{o}C. A constitutive model based on Gibbs free energy is developed to predict the behavior of this material. Two different irrecoverable strains including transformation induced plastic strain (TRIP) and viscoplastic strain (VP) are considered when using high temperature shape memory alloys (HTSMAs). The first one happens during transformation at high levels of stress and the second one is related to the creep which is rate-dependent. The developed model is implemented for NiTiHf under uniaxial loading. Finite difference method is utilized to solve the proposed equations. The material parameters in the equations are calibrated from experimental data. Simulation results are captured to investigate the superelastic behavior of NiTiHf. The extracted results are compared with experimental tests of isobaric heating and cooling at different levels of stress and also superelastic tests at different levels of temperature. More results are generated to investigate the capability of the proposed model in the prediction of the irrecoverable strain after full transformation in HTSMAs.

Keywords: High temeperature shape memory alloys, NiTiHf, uniaxial loading, analytical solution, finite difference method

1. INTRODUCTION

NiTi, as the most well-known Shape memory alloy (SMA) shows two distinct behaviors: superelastic (SE) and shape memory effect (SME). These behaviors are due to the phase transformation that happens in the material between martensite and austenite, which have different lattice structures. The material shows SE when it is in the austenite phase. At this region, the material can recover up to 8% of stress-induced strain. However, SME occurs when the material is in the martensite region, where stress-induced strain is recovered by heating the material up to the austenite phase. NiTi has received more attraction because of its ductility, compatibility, and stability which results in their application in biomedical devices and actuators[1].

The transformation temperatures of NiTi are in the order of room temperature which limits their application in industries like automotive and aerospace, where the operating temperatures are in the order of 100^{o}C or more. Researchers have solved this problem by adding a third element to NiTi-based SMAs like Palladium (Pd), Hafnium (Hf) and Zirconium (Zr), and the resultant material is called "high temperature shape memory alloy (HTSMA)"[2, 3]. This third element can increase the transformation temperatures of the material significantly, and make them applicable to high temperature applications like aerospace and energy exploration industries[4]. Comparing these third elements, Hf and Zr are less expensive and less amount is needed to increase the transformation temperatures sufficiently. Furthermore, NiTiHf and NiTiZr are not exposed to creep, which is a problem with using the materials at high temperatures, since creep is activated when the temperature of the material is 0.3-0.4 melting temperature, and melting temperature of NiTiHf and NiTiZr are very high compared to their transformation temperatures [5]. Bigelow et al.[6] have studied Ni-rich NiTiHf and showed that this alloy is very stable and superelastic at high temperatures. Exposing to the high temperatures, two more strains occur in SMAs; one is a viscoplastic strain which is related to creep, and the other is transformation-induced plastic (TRIP) strain which is related to the phase transformation.

*mohammad.elahinia@utoledo.edu; phone 1 419 530-8224; fax 1 419 530-8206; http://www.eng.utoledo.edu/~melahini/

Behavior and Mechanics of Multifunctional Materials and Composites XII,
edited by Hani E. Naguib, Proc. of SPIE Vol. 10596, 1059613 · © 2018 SPIE
CCC code: 0277-786X/18/$18 · doi: 10.1117/12.2300857

Karaca et al.[7] investigated the superelastic behavior of single crystal NiTiHf, as well as thermal cyclic tests and they showed a good superelasticity for this material under temperatures up to 200°C. Different phenomenological modeling works have been done on SMAs, which are based on the continuum thermodynamics principles [8-12]. Lagoudas and Entchev[13] entered the transformation-induced plasticity (TRIP) into their model for SMAs at high levels of stress. This model is also improved for HTSMAs by entering viscoplastic strain to the equations. The material that they used was NiTiPd which is sensitive to creep at high temperatures. Finite element method (FEM) is conducted with most of these modeling works.

In this study we present a semi-analytical approach, based on Gibbs free energy, to model the mechanical behavior of NiTiHf under uniaxial loading. For solving the equations finite difference method (FDM) is utilized, which is simpler in implementation and numerically less expensive, comparing to FEM. This method has been done for SMAs by Mirzaeifar et al.[8] and Andani et al.[14]. Here, it is improved for HTSMAs and then applied to NiTiHf under uniaxial loading. The model is also verified with experimental data and a good agreement is observed. Using this model, the plastic strain, which remains as the residual strain in the material is predictable.

2. GOVERNING EQUATIONS

2.1 General constitutive model

The model is based on the Gibbs free energy and it is implemented by Boyd and Lagoudas[10], and Qidwai and Lagoudas[15]. For HTSMAs, as explained above, two more strain terms are added: viscoplastic strain and transformation-induced plastic strain.

$$\begin{aligned} G(\sigma, \varepsilon^t, \varepsilon^{tp}, \varepsilon^{vp}, T, \xi, p) &= \frac{-1}{2\rho}\sigma{:}S{:}\sigma - \frac{1}{\rho}\sigma{:}[\alpha{:}(T-T_0) + \varepsilon^t + \varepsilon^{tp} + \varepsilon^{vp}] + c\left[(T-T_0) - T ln\left(\frac{T}{T_0}\right)\right] - s_0 T \\ &+ u_0 + \frac{1}{\rho}[g^t(\xi) + g^{vp}(T,p)] \end{aligned} \tag{1}$$

Where ρ, S, α, c, s_0, u_0, $\sigma, \varepsilon^t, \varepsilon^{tp}, \varepsilon^{vp}, T, \xi$, p, g^t and g^{vp} are material mass density, effective compliance tensor, thermal expansion coefficient, specific heat, specific entropy, specific internal energy in the initial state, stress, transformation-induced strain, transformation-induced plastic strain, viscoplastic strain, temperature, martensitic volume fraction, effective viscoplastic strain, transformation and viscoplastic hardening functions, respectively [16]. The total strain can be defined as:

$$\epsilon^{total} = -\rho\frac{\partial G}{\partial \sigma} = S{:}\sigma + \alpha{:}(T-T_0) + \varepsilon^t + \varepsilon^{tp} + \varepsilon^{vp} \tag{2}$$

Where

$$\dot{\varepsilon}_t = \Lambda^t\dot{\xi}, \quad \dot{\varepsilon}_{tp} = \Lambda^{tp}\dot{\xi}, \quad \dot{\varepsilon}_{vp} = \Lambda^{vp}\dot{p} \tag{3}$$

Λ^t, Λ^{tp}, Λ^{vp} and $\dot{p}$, the rate of viscoplastic strain, are expressed as:

$$\Lambda^t = \begin{cases} \frac{3}{2}H\frac{\acute{\sigma}}{\bar{\sigma}} \ (\dot{\xi} > 0) \\ \frac{\varepsilon^{t-r}}{\xi^{t-r}} \ (\dot{\xi} < 0) \end{cases}, \quad \Lambda^{tp} = \begin{cases} f^{tp}(\sigma)\Lambda^{vp} \ (\dot{\xi} > 0) \\ -f^{tp}(\sigma)\Lambda^{vp} \ (\dot{\xi} < 0) \end{cases}, \quad \Lambda^{vp} = \frac{3}{2}\frac{\acute{\sigma}}{\bar{\sigma}}, \ \dot{p} = \exp\left(\frac{-Q}{RT}\right)\bar{\sigma}^{N_a} \tag{4}$$

H, $\acute{\sigma}$, $\bar{\sigma}$, ε^{t-r}, ξ^{t-r}, f^{tp}, Q, R, and N_a are the maximum recoverable strain, deviatoric part of the stress tensor, the effective stress, transformation strain at the reversal, martensitic volume fraction at the reversal, the TRIP strain generation rate at a given stress and three material constants, respectively. The Clausius-Durham inequality is defined as [17]:

$$\left[\sigma:(\Lambda^t+\Lambda^{tp})-\rho\frac{\partial G}{\partial\xi}-g^t(\xi)\right]\dot{\xi}=\pi^t\dot{\xi}>0\ \ \forall\dot{\xi}\neq 0 \tag{5}$$

$$[\sigma:\Lambda^{vp}-f^{vp}(p,T)]\dot{p}=\pi^{vp}\dot{p}>0\ \ \forall\dot{p}>0 \tag{6}$$

π^t and π^{vp} are thermodynamic forces, and transformation and viscoplastic hardening functions are defined as:

$$g^t=\begin{cases}\frac{1}{2}\rho b^M\xi^2+(\mu_1+\mu_2)\xi & \dot{\xi}>0\\ \frac{1}{2}\rho b^A\xi^2+(\mu_1-\mu_2)\xi & \dot{\xi}<0\end{cases} \tag{7}$$

$$g^{vp}=\dot{p}f^{vp}(p,T) \tag{8}$$

$\rho b^M,\rho b^A,\mu_1$ and μ_2 are material constants. The transformation function showing the state of the material is expressed as [8].:

$$\phi^t=\begin{cases}\pi^t-Y^t=0 & \dot{\xi}>0\\ -\pi^t-Y^t=0 & \dot{\xi}<0\\ <0 & \dot{\xi}=0\end{cases} \tag{9}$$

Y^t is a threshold value for the thermodynamic force. The transformation function (ϕ^t) shows the state of the phase transformation; when the material is not during phase transformation, the value of the transformation function is less than zero. When the material is in forward ($\dot{\xi}>0$) or reverse transformation ($\dot{\xi}<0$), the value is zero[8].

2.2 Relations for uniaxial loading

For the case of uniaxial loading, the explicit expression for martensitic volume fraction in forward and reverse transformation can be obtained as:

$$\xi^{fwd}=\frac{1}{\rho b^M}[\big(H+f^{tp}(\sigma)\big)\sigma_z+\frac{1}{2}\sigma_z^2\Delta S_{33}+\rho\Delta c\left[(T-T_0)-Tln\left(\frac{T}{T_0}\right)\right]+\rho\Delta s_0(T-M_s)] \tag{10}$$

$$\xi^{rev}=\frac{1}{\rho b^A}[\frac{\sigma_z\epsilon_{zz}^{t-r}}{\xi^{t-r}}+f^{tp}(\sigma)\sigma_z+\frac{1}{2}\sigma_z^2\Delta S_{33}+\rho\Delta c\left[(T-T_0)-Tln\left(\frac{T}{T_0}\right)\right]+\rho\Delta s_0\big(T-A_f\big)] \tag{11}$$

Δ(variable) shows the difference between martensite and austenite values of the variables. The material parameters in the equations above are:

$$\mu_1=\tfrac{1}{2}\,\rho\Delta s_0\big(M_s+A_f\big)-\rho\Delta u_0,\ \ \mu_1=\tfrac{1}{2}(\rho b^A-\rho b^M),$$
$$\rho b^A=-\rho\Delta s_0\big(A_f-A_s\big),\rho b^M=-\rho\Delta s_0\big(M_s-M_f\big),Y^t=-\tfrac{1}{2}\,\rho\Delta s_0\big(A_f-M_s\big) \tag{12}$$

Using equations (10), (11), (2) and (3), the uniaxial strain for forward and reverse transformation is obtained:

$$\epsilon_z^{fwd} = \frac{1}{E_A + \xi^{fwd}(E_M - E_A)}\sigma_z + \left(H + f^{tp}(\sigma)\right)\xi^{fwd} + \alpha(T - T_0) + \exp\left(\frac{-Q}{RT}\right)\sigma_z^{N_a} \quad (13)$$

$$\epsilon_z^{rev} = \frac{1}{E_A + \xi^{rev}(E_M - E_A)}\sigma_z + \frac{\epsilon_z^{t-r}}{\xi^{t-r}}\xi^{rev} + f^{tp}(\sigma)\xi^{rev} + \alpha(T - T_0) + \exp\left(\frac{-Q}{RT}\right)\sigma^{N_a} \quad (14)$$

As discussed in the introduction section, creep is negligible for NiTiHf at the temperatures and stresses of operation, due to the fact that the operation temperature of this material is less than 0.35 melting temperature, where creep comes into play. Therefore, viscoplastic strain term can be considered as zero.

3. SOLUTION METHOD

To solve the obtained equations, an iterative solution is considered. Finite difference method (FDM) as a MATLAB code is employed which has some benefits to the FEM, as mentioned above. The circular cross section is divided into N annular elements, as shown in Figure1, and for each element the stress or temperature is calculated based on the implemented equations. The input is strain which is applied to the material in M steps. Therefore, the axial and torsional strains for each element are obtained:

$$\epsilon_z = \frac{\text{axial displacement}}{\text{length of the sample} * \text{total number of steps}} * \text{number of current step} \quad (15)$$

4. RESULTS

The capability of the model is verified by the experimental results reported by the third author [7] for uniaxial loading condition. The samples used for these experiments were cubes 4*4*8 mm under uniaxial compression, and the composition was $Ni_{50.3}Ti_{29.7}Hf_{20}$ with [1 1 1] orientation. The superelastic and thermal cyclic behaviors of the material are considered to be isothermal and isobaric, respectively. Therefore, since the strain is uniform along the cross section, it is possible to use the model for rectangular samples, as well. Table 2 describes the material properties of the tested samples. H and f^{tp} are the maximum transformation strain after accounting for elastic moduli and the irrecoverable strain, respectively, and they are found from the cyclic heating and cooling tests. E_A and E_M are the austenite and martensite elastic modulus, respectively, and they are obtained from the stress-strain curves at the austenite and martensite phases (the slope of the plot at each region). C_M and C_A are calibrated from the phase diagram of the material.

Two different sets of results are investigated for validation: isobaric thermally cyclic behavior and isothermal superelastic behavior. Figure 1 and 2 are isobaric cooling and heating results at 100 and 1000 MPa, respectively. As reported in the experimental work [7], the irrecoverable strain is negligible for the stress levels less than 700MPa. Figure 3 and 4 show the superelastic behavior of NiTiHf at different temperatures of 180°C and 200°C, respectively. The difference between model and experimental results is mostly due to the approximation of f^{tp} function, because of the few number of experimental results for curve fitting. In our future work, we plan to do more experimental tests of isobaric thermal cycling to present a more accurate function. Superelastic behavior at different temperatures are modeled to show the effect of temperature for the same amount of transformation (Figure 5). It is obvious that increasing the temperature, the material goes through higher levels of stress which results in more transformation-induced plasticity which remains as a plastic strain after unloading.

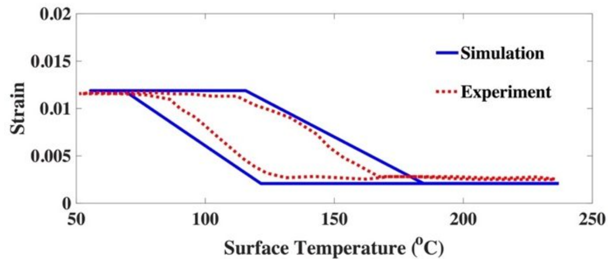

Figure 1. Thermal cyclic behavior under constant stress=100MPa

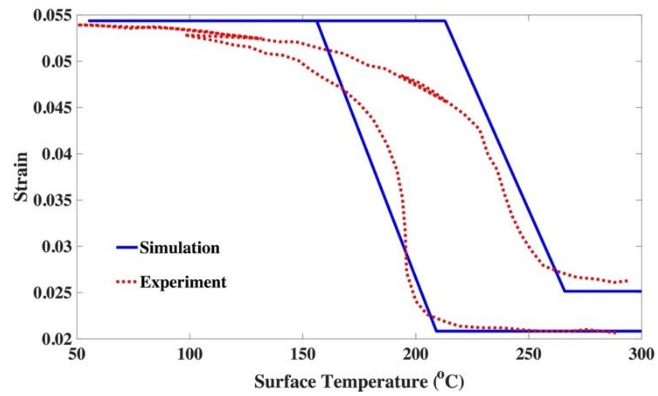

Figure 2. Thermal cyclic behavior under constant stress=1000MPa

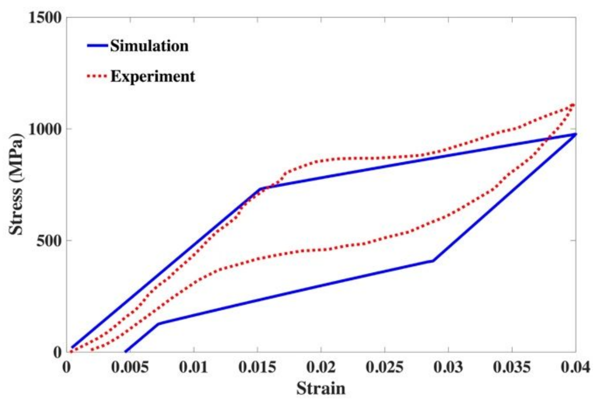

Figure 3. Superelastic behavior of NiTiHf at temperature=180^{o}C

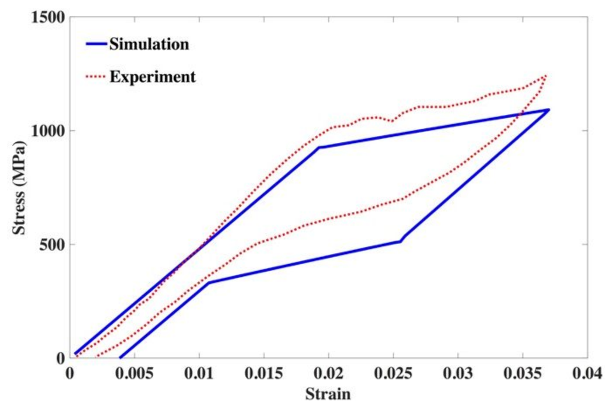

Figure 4. Superelastic behavior of NiTiHf at temperature=200^{o}C

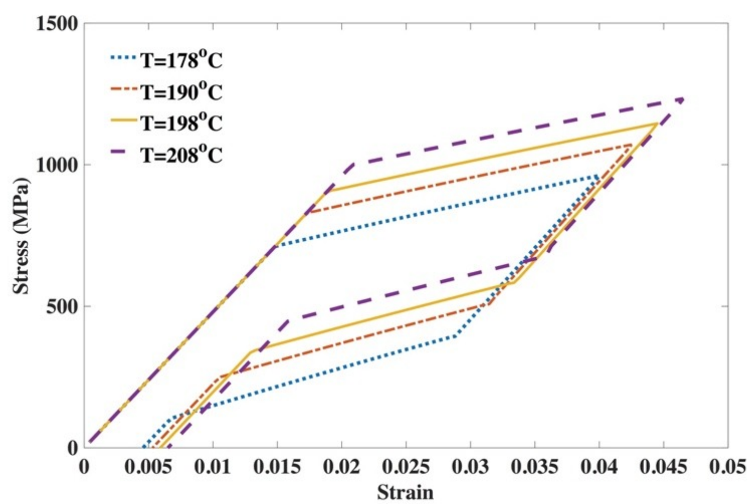

Figure 5. Superelastic behavior of NiTiHf at different temperatures for the same amount of transformation

5. CONCLUSION

A semi-analytical model is improved to simulate the superelastic and thermal cyclic behavior of HTSMAs. Transformation-induced plastic strain and viscoplastic strain enters the equations, due to high stress levels, when operating at high temperatures. The solution method utilized to solve the equations is finite difference method. The results are compared with the experimental data on NiTiHf samples under uniaxial loading. Using this model, the residual strain in NiTiHf is predictable at different levels of temperatures.

REFERENCES

[1] M. Elahinia, [Shape memory alloy actuators: design, fabrication and experimental evaluation] John Wiley & Sons, (2015).

[2] J. H. Mulder, [Investigation of High Temperature Shape Memory Alloys from the Ni-Ti-Zr and Ni-Ti-Hf Systems] Univ. Twente, (1995).

[3] D. N. AbuJudora, P. E. Thoma, M. Y. Kao *et al.*, [High transformation shape memory alloy], US(1992).

[4] J. Ma, I. Karaman, and R. D. Noebe, "High temperature shape memory alloys," International Materials Reviews*,* 55(5), 257-315 (2010).

[5] C. M. Denowh, and D. A. Miller, "Thermomechanical training and characterization of Ni–Ti–Hf and Ni–Ti–Hf–Cu high temperature shape memory alloys," Smart Materials and Structures*,* 21(6), (2012).

[6] G. S. Bigelow, A. Garg, I. I. Padula *et al.*, "Load-biased shape-memory and superelastic properties of a precipitation strengthened high-temperature Ni50.3Ti29.7Hf20 alloy," Scripta Materialia*,* 64(8), 725-728 (2011).

[7] H. E. Karaca, S. M. Saghaian, B. Basaran *et al.*, "Compressive response of nickel-rich NiTiHf high-temperature shape memory single crystals along the [111] orientation," Scripta Materialia*,* 65(7), 577-580 (2011).

[8] R. Mirzaeifar, R. DesRoches, and A. Yavari, "Analysis of the rate-dependent coupled thermo-mechanical response of shape memory alloy bars and wires in tension," Continuum Mechanics and Thermodynamics*,* 23(4), 363-385 (2011).

[9] L. C. Brinson, "One-dimensional constitutive behavior of shape memory alloys: thermomechanical derivation with non-constant material functions and redefined martensite internal variable," Journal of Intelligent Material Systems and Structures 4(2), 229–242 (1993).

[10] J. G. Boyd, and D. C. Lagoudas, "A thermodynamical constitutive model for shape memory materials. Part I. The monolithic shape memory alloy," International Journal of Plasticity*,* 12(6), 805–842 (1996).

[11] R. Mehrabi, M. Kadkhodaei, M. T. Andani *et al.*, "Microplane modeling of shape memory alloy tubes under tension, torsion, and proportional tension–torsion loading," Journal of Intelligent Material Systems and Structures*,* 26(2), 144-155 (2015).

[12] R. Mehrabi, M. Kadkhodaei, and M. Elahinia, "A thermodynamically-consistent microplane model for shape memory alloys," International Journal of Solids and Structures*,* 51(14), 2666-2675 (2014).

[13] D. C. Lagoudas, and P. B. Entchev, "Modeling of transformation-induced plasticity and its effect on the behavior of porous shape memory alloys. Part I: constitutive model for fully dense SMAs," Mechanics of Materials*,* 36(9), 865-892 (2004).

[14] M. T. Andani, A. Alipour, A. Eshghinejad *et al.*, "Modifying the torque–angle behavior of rotary shape memory alloy actuators through axial loading: A semi-analytical study of combined tension–torsion behavior," Journal of Intelligent Material Systems and Structures*,* 24(12), 1524-1535 (2013).

[15] M. A. Qidwai, and D. C. Lagoudas, "Numerical implementation of a shape memory alloy thermomechanical constitutive model using return mapping algorithms," International Journal for Numerical Methods in Engineering*,* 47(6), 1123–1168 (2000).

[16] D. J. Hartl, G. Chatzigeorgiou, and D. C. Lagoudas, "Three-dimensional modeling and numerical analysis of rate-dependent irrecoverable deformation in shape memory alloys," International Journal of Plasticity*,* 26(10), 1485-1507 (2010).

[17] L. Anand, and M. E. Gurtin, "Thermal effects in the superelasticity of crystalline shape-memory materials," Journal of the Mechanics and Physics of Solids 51, 1015–1058 (2003).